Reprinted from:
THE REVIEW OF SCIENTIFIC INSTRUMENTS VOLUME 43, NUMBER 1 JANUARY 1972

Design Parameters for the Cylindrical Mirror Energy Analyzer*

JOHN S. RISLEY†
Department of Physics, University of Washington, Seattle, Washington 98105
(Received 22 July 1971; and in final form, 13 September 1971)

Design parameters are presented for various geometrical arrangements of the cylindrical mirror electron energy analyzer. The theory and operation of this high quality instrument are discussed and compared with an experimental device. Similar properties of a parallel plate analyzer with second order focusing are reviewed.

INTRODUCTION

The cylindrical mirror electron-energy analyzer has the primary advantage that its cylindrical symmetry insures that all entering electrons which pass through the cylinders' coaxis will again be focused on the coaxis after leaving the analyzer, making it possible to use the complete 2π azimuthal angle. This focusing property is extremely useful in collision experiments where a narrow beam of particles (photons, electrons, or ions) collides with a gaseous target producing secondary energetic particles along a well-defined axis. Furthermore, the cylindrical mirror analyzer can be designed to have the unusual feature of accepting electrons which have a relatively large spread in entrance angles without suffering a large degradation in resolution. That is, for a given energy resolution determined by the finite size of the source and the exit slitwidth, monoenergetic electrons with a large spread in entrance angles will be transmitted or focused through the analyzer. The entrance angle is defined by the initial electron path and the axis of the analyzer. On the other hand, entering electrons having energies which differ from the specific electron energy being analyzed are dispersed quite well. For two analyzers of comparable dimensions, i.e., the same sized source and exit slit and the same separation between the entrance and exit slits, the one with larger energy dispersion will have a higher energy resolution.

The equation for the trajectory of an electron passing through the analyzer is discussed in the next section. Also an expression for the energy resolution is derived in order to establish the criteria for good design parameters. The choice was based on achieving the maximum electron transmission for a given entrance angle spread with the least degradation in the energy resolution. In some experiments, however, the range of entrance angles is restricted sufficiently by a set of apertures so that optimum transmission is not necessary, allowing one considerable freedom in choosing the mean entrance angle. A wide range of entrance angles is especially important in beam collision experiments designed to accept the total azimuthal angle and also designed to measure the relative heights of electron spectral lines at different angles.

Since the cylindrical mirror analyzer has definite advantages, e.g., complete azimuthal acceptance angle, high order focusing, and high resolving power, it is felt that the cylindrical mirror analyzer would be in wider use were it not for the difficulties involved in calculating the design parameters from the equations of motion. Therefore, the expression for the trajectory of an electron inside the analyzer, which cannot be solved analytically, was evaluated numerically in order to extract the design parameters for constructing practical analyzers. Presented below is a table of the design parameters for the optimum focusing configuration and several parametric graphs for the next best transmission condition. These results are more accurate and more extensive than the previous calculations of Zashkvara and Red'kin[1] and Aksela *et al.*,[2] who gave illustrative graphs and tables for a limited range of source image positions. Sar-El[3] and Zashkvara *et al.*[4] dealt only with the case where the source and image were positioned along the cylinders' coaxis. Our parametric graphs provide new results which will allow greater design freedom. Also, in the last section of this paper the measured energy resolution of our experimental cylindrical mirror analyzer is shown to agree quite well with the predicted resolution.

REVIEW OF PREVIOUS INVESTIGATIONS

Theoretical

Although an experimental version of this analyzer was reported as early as 1952,[5] theoretical descriptions of the angular focusing were not written until the mid-1960's by Zashkvara *et al.*[4] and Sar-El.[3] Sar-El extended his treatment to relativistic particles.[6] Zashkvara and Red'kin[1] and Aksela *et al.*[2] discussed the freedom one has in choosing the location of both the electron source and its image while maintaining its high degree of focusing. This property was independently discovered in our laboratory during the analysis of our experimental cylindrical mirror analyzer, shown schematically in Fig. 1, which was designed using Sar-El's parameters.[3] In our case, the cylinders were only partial in order to allow an electron beam to enter the analyzer. The source of the beam was located far away from the analyzer. The analyzer fringing fields were reduced by using electrodes inserted between the outer edges of the two cylinders and set at the appropriate potentials to maintain the radial electric field inside the analyzer.

Previously the concentric spherical deflector analyzer[7] was considered the best electrostatic analyzer known; how-

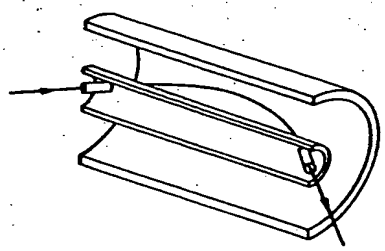

FIG. 1. Experimental arrangement, shown schematically, of the electrostatic, cylindrical mirror electron-energy analyzer.

ever, Hafner *et al.*[8] found that the cylindrical mirror analyzer had significantly superior focusing and dispersion. Lately, Sar-El proposed a new figure of merit in order to compare various types of analyzers.[9] Sar-El's figure of merit is proportional to the transmission of a diverging beam of monoenergetic electrons incident on the analyzer entrance aperture. The transmission is directly related to the solid angle of the beam accepted by the analyzer and is also a function of the analyzer energy resolution. Using Sar-el's results, one finds that for an analyzer with an energy resolution less than 30% (ratio of the full width at half-maximum to the mean electron energy) the cylindrical mirror analyzer is better than the spherical deflector. High quality analyzers have resolving powers which are much higher than this, i.e., a good analyzer should be able to resolve two peaks in an energy spectrum that are separated by less than 5–10% of the mean electron energy. Our experimental analyzer, for example, had a resolution of $\frac{1}{2}$%.

Recently, Green and Proca[10] reported a new focusing design for the parallel plate analyzer. Since its focusing properties are similar to the cylindrical mirror analyzer, their results are reviewed below.

Experimental

Several experimental versions of the cylindrical mirror analyzer have been reported. Blauth[11] used a design that analyzed secondary electrons which were emitted at 54.5° from the coaxis. Since the electron source and image were close to the inner cylinder, the maximum angular focusing was not practical and only first order focusing was realized. Mehlhorn[12] used this same design for his extensive Auger spectroscopy measurements. Ogurtsov, Flaks, and Avakyan[13] described a method for observing electrons ejected at angles other than 54.5° by placing an additional transparent cylinder between the axis and the inner cylinder and applying a potential to it to deflect the electron trajectories. They claim a practical range of 30–75°; however, no angular distribution measurements have yet been reported.[14]

Recently Harting[15] described a method where, by using the cylindrical mirror analyzer, angular distribution measurements could be made without the need of mechanically rotating any apparatus inside the vacuum chamber. An electron gun was placed at right angle to the cylinders' coaxis and six sets of entrance and exit slits were cut around the inner cylinder corresponding to scattering angles every 20° between 40 and 140°. Electrons, which were emitted from a point where the electron beam and target particles intersected, passed into the analyzer. The entrance angle (the same for all electrons) was 51°. As with the above versions, the source and image were assumed to lie on the inner cylinder and first order angular focusing was employed. Since electrons from all angles, defined by the entrance and exit slit, were analyzed, six separate electrodes were placed immediately before the particle multiplier. A potential could be applied to each electrode in order to deflect the electrons away from the particle multiplier, thus allowing electrons from each angle to be detected separately. In this version, the azimuthal symmetry of the cylindrical mirror analyzer was exploited for angular distribution measurements rather than for a larger azimuthal acceptance angle.

The experimental apparatus of Vassilev, Baudon, Rahmat, and Barat[16] utilized second order focusing to observe scattered ions between 3 and 19°. The scattered ions were deflected by a conical electrostatic mirror which transformed the slope of the initial trajectories to 34 and 50° respectively. The large spread of ±9° around the mean entrance angle of 42° can be accommodated by the cylindrical mirror analyzer when designed for second order focusing.

PARTICLE DYNAMICS

Theory

Figure 2 defines the geometrical parameters for this analysis. The electrons with kinetic energy E (eV) are assumed to pass through the coaxis (the z axis) before entering the analyzer at an entrance angle θ. This assumption implies, of course, that the electron angular momentum is zero about the z axis, and greatly simplifies the equations of motion. The case for electrons which pass close to, but not through the z axis is considered in a subsequent section in this paper. Once the electrons enter the analyzer, they are deflected to the inner cylinder by the voltage V_d on the outer cylinder of radius b. If this voltage is chosen correctly, the electrons travel in an arc and leave the analyzer continuing in a straight line to the image located at d_i. If the exit slit has a finite width, then electrons with energies slightly different than E will also pass through the exit slit. (It is assumed in this analysis that the location of the exit slit defining the resolution coincides with the image.) Likewise, the finite size of the electron source produces an analogous effect. The entrance slit, which defines the mean entrance angle and the angular spread, can be placed anywhere between the electron source at d_s and the inner cylinder. Also, electrons with the same energy but with a spread in entrance angles can also pass through the exit slit. However, the resolution can be de-

graded by this angular effect since electrons with different energies but with the correct combination of energy and entrance angle can be deflected through the exit slit. By solving the equations of motion the electron trajectory and the resolution can be predicted.

Trajectory

The equation of motion for the electrons' radial trajectory inside the analyzer (with zero angular momentum) is

$$m\ddot{r} = -[V_d/\ln(b/a)]1/r, \tag{1}$$

where r is the radial distance from the z axis. From this, one can find (see Ref. 3, for example) the total distance along the z axis that the electrons with energy E travel from source to image,

$$z_0 = (d_s+d_i)\cot\theta + 4ak^{\frac{1}{2}}\cos\theta e^{k\sin^2\theta}\int_0^{\sqrt{k}\sin\theta} e^{-u^2}du, \tag{2}$$

where $k=(E/V_d)\ln(b/a)$. Only the total distance from the source and the image to inner cylinder is important, i.e.,, d_s+d_i; thus the electron source and image can be placed in any asymmetrical configuration for a particular $d=d_s+d_i$. Since the maximum radial range from the z axis for the electrons inside the analyzer is

$$r_m = a\exp(k\sin^2\theta), \tag{3}$$

the calibration constant $C=V_d/E$ must be larger than $\sin^2\theta$ to prevent the electrons from hitting the back deflection plate.

Diffuse Source

Occasionally there is an ambiguity in defining the cylindrical source, and consequently the distance d_s. For a small surface emitting photoelectrons or thermionic electrons, d_s is the perpendicular distance from the inner cylinder to the emitting surface. The size of the electron source is simply that portion of the surface where electrons are created which pass into the analyzer. However, in most collision experiments the electron source is defined by two apertures which collimate a diffuse source of electrons. The two apertures, shown schematically in Fig. 3, define a penumbra in the collision region whose limit is indicated by two lines, each of which passes from one edge of one aperture to the opposite edge of the other aperture. The point at which these lines cross locates d_s for a diffuse electron source. Furthermore, when dealing with a diffuse electron source the effective size of the source is determined by the two apertures. If the widths of the two apertures are denoted by w_1 and w_2 and if l_1 and l_2 are, respectively, the perpendicular distances from apertures 1 and 2 to the crossing point, then the effective size w_s of the source is found using the expression

$$w_s = (l_2w_1+l_1w_2)/(l_1+l_2). \tag{4}$$

However, if the aperture closest to the inner cylinder is the smaller of the two, then the effective size of the electron source is equal to the width of the smaller aperture.

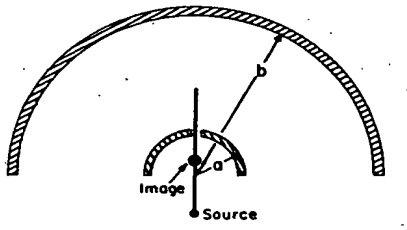

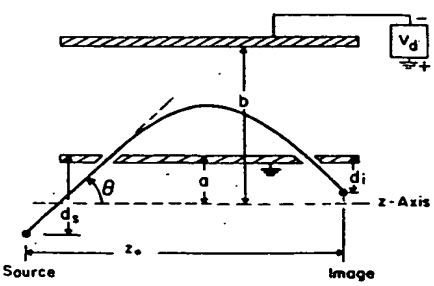

FIG. 2. Electron trajectory inside a cylindrical mirror energy analyzer. Top, end-on view view; bottom, side view.

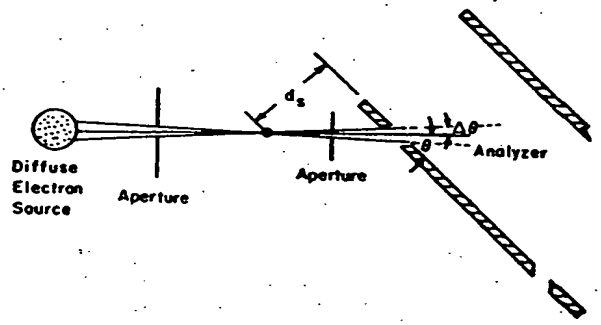

FIG. 3. Schematic representation of the electron source defined by two apertures collimating a diffuse electron beam.

RESOLUTION

Taylor's Expansion

The resolution of an analyzer is conveniently described analytically by the base resolution. The base resolution is defined as the width of a spectral line measured at its base divided by the mean energy of the peak. In order to predict how far electrons with incorrect energy or entrance angle will either overshoot or undershoot the distance z_0 from source to image, one expands the distance in a Taylor's series about both a variation in energy ΔE and in entrance angle $\Delta\theta$,

$$z = z_0 + \sum_{n=1}^{\infty}\frac{1}{n!}\left(\Delta\theta\frac{\partial}{\partial\theta}+\Delta E\frac{\partial}{\partial E}\right)^n z(\theta,E)\Big|_{\theta=\theta_0,E=E_0}, \tag{5}$$

where $\Delta\theta=\theta-\theta_0$ and $\Delta E=E-E_0$;

$$z=z_0+\sum_{i=1}^{\infty}\frac{1}{i!}\frac{\partial^i z}{\partial\theta^i}\bigg|_{z_0}(\Delta\theta)^i+\sum_{j=1}^{\infty}\frac{1}{j!}\frac{\partial^j z}{\partial E^j}\bigg|_{z_0}(\Delta E)^j + \sum_{i,j=1}^{\infty}\frac{c_{ij}}{(i+j)!}\frac{\partial^{i+j}z}{\partial\theta^i\partial E^j}\bigg|_{z_0}(\Delta\theta)^i(\Delta E)^j, \quad (6)$$

where c_{ij} is the binomial expansion coefficient. The first series in Eq. (6) gives the degradation in resolution due to entering electrons with a finite spread in entrance angles. The individual terms in this series correspond to the degree of focusing associated with an analyzer. If the first partial derivative is zero, then one has first order focusing. High quality analyzers usually satisfy this condition. The unexpected result is that the cylindrical mirror analyzer can also have second order focusing since the various geometrical relationships can be chosen so that the second derivative equals zero.

Dispersion

The base resolution $R=\Delta E/E$ is found by inverting Eq. (6). Since most of the terms in Eq. (6) are negligible compared to $(\partial z/\partial E)\Delta E$, this inversion procedure is greatly simplified. The linear energy dispersion is found from the first term of the second series. The dispersion is defined by

$$D=E\partial z/\partial E. \quad (7)$$

The cross terms are neglected because they are always much smaller (by a factor of $\Delta E/E$) than any remaining terms.

Angular Aberrations

Before an expression for the resolution can be written, consideration must be made, in the first series, for the fact that odd ordered terms will produce exactly twice as much separation in the z direction as will the even terms. That is, if one writes

$$\Delta z(\Delta\theta)=\sum_{i=1}^{\infty}\frac{1}{i!}\frac{\partial^i z}{\partial\theta^i}\bigg|_{z_0}(\Delta\theta)^i, \quad (8)$$

then the sign of the even terms in the series will be the same for both positive and negative $\Delta\theta$, while the sign for the odd terms will be the opposite. Therefore, when calculating the total variation $\Delta z_T(+\Delta\theta, -\Delta\theta)$ in the trajectory along the z axis, the direction in which Δz increases for both positive and negative acceptance angle spreads must be taken into account. If $\Delta z(+\Delta\theta)$ and $\Delta z(-\Delta\theta)$ are in the same direction, that is, if they have the same sign, then the total Δz_T is equal to the absolute value of the larger of $\Delta z(+\Delta\theta)$ or $\Delta z(-\Delta\theta)$. If $\Delta z(+\Delta\theta)$ and $\Delta z(-\Delta\theta)$ are in the opposite direction (have opposite signs) then $\Delta z_T=|\Delta z(+\Delta\theta)-\Delta z(-\Delta\theta)|$.

Exit Slit Effect

There is a direct correspondence between the spread Δz as expressed in Eq. (6) and the artificially induced spread due to the size of the source and the finite exit slit. One must be careful to use the correct geometrical projections of the slit (or source) when calculating the resolution. The slit projection must, of course, be in the same direction as the dispersion, i.e., along the z axis. Therefore, the correct length is the elongated one which is found by projecting the slitwidth along the mean direction of the electron beam to the z axis. That is, if an exit slit w_e is placed normal to the electron path, the z component of the exit width w_e is

$$w_{e_z}=w_e/\sin\theta. \quad (9)$$

Finite Source

The effect of the finite size of the electron source which also degrades the resolution can be best considered by dividing the problem into two parts: those electrons which pass through the z axis but are distributed along the axis, and those electrons which have a straight line trajectory passing by the axis at some distance of closest approach.

Electrons Passing through the Axis

That part of the source which is extended along the z axis only increases the resolution in the same manner as the exit slit,[17]

$$R(w_{s_z})=w_{s_z}/D, \quad (10)$$

where w_{s_z} is the length of the source along the z axis.

Off-Axis Electrons

The off-axis electrons are assumed to pass by the z axis at a distance of closest approach r_c. By conservation of angular momentum after the electrons are deflected by the radial field between the cylinders, they will again pass by on the opposite side of the z axis at a distance of closest approach r_c. If the ratio of r_c to the inner cylinder radius is small, then the two points of closest approach and the z axis will almost lie in the same plane. Since only the radial part of the kinetic energy will be analyzed and since this is less than the kinetic energy of the electrons which pass through the axis, the off-axis electrons will fall short of the image point d_i. The radial part of the kinetic energy for electrons entering at θ is

$$E_r=[1-(r_c/a)^2]E\sin^2\theta. \quad (11)$$

Therefore, the expression for the degradation of the resolution due to off-axis electrons is

$$R(r_c)=(r_c/a)^2. \quad (12)$$

Base Resolution

Using the above expressions, Eq. (6) can be solved approximately for the base resolution,

$$R \approx \frac{w_{s_z}+w_{e_z}}{D}+\left(\frac{r_c}{a}\right)^2+\frac{\Delta z_T(+\Delta\theta,-\Delta\theta)}{D}, \qquad (13)$$

where w_{s_z} is the effective size of the electron source along the z axis, w_{e_z} is the projected exit slit width along the z axis, and D is the dispersion. To achieve the optimum analyzer design (the highest transmission along with the highest resolving power) one usually equates the first and third terms in Eq. (13).[17]

Explicit expressions for the first three partial derivatives with respect to θ, the aberration constants, and for the dispersion are listed in the Appendix.

Minimum Beamwidth

The smallest width of the deflected electron beam does not occur exactly in the image plane when second order focusing is achieved. Hafner *et al.*[8] and Aksela *et al.*[2] have pointed out that since the third partial derivative is negative, the minimum width occurs slightly before the beam comes to a focus at the image plane. The position of this minimum width depends directly on the entrance angle spread. For $d=2a$ and $\Delta\theta=\pm 6°$, the position is less than $0.1a$ from the z axis. This is a relatively small correction which decreases in importance when the finite size of the electron source is taken into account.[2] Recently, Aksela[18] compared in detail the energy distribution of electrons transmitted through a cylindrical mirror analyzer at the location of both the minimum trace width and the image of the second order focus. When the effect of a large divergence in entrance angles is greater than the effect due to the size of the slitwidths, that is, when the third term in Eq. (13) is much larger than the first, Aksela found that the base width of the energy distribution was smaller at the minimum width location; however, the FWHM was significantly smaller at the second order focus. Furthermore, the distribution at the minimum width exhibited two sharp peaks. These double peaks could produce serious complications in spectrum analysis. When the effect due to the size of the source and exit slit is not negligible, then the double peaks are smoothed out and the FWHM for both distributions are comparable. Proca and Green[19] reported similar results for the parallel plate analyzer with second order focusing.

ANALYZER ENERGY CALIBRATION CONSTANT

The calibration constant for an energy analyzer can be set arbitrarily. If $V_d/E=C$ is set equal to unity, the analyzer deflection voltage will correspond directly to the energy making it convenient to identify lines in energy spectra. Also, if a constant analyzing voltage is used, that is, if the voltage between the outer cylinder and the inner cylinder is held constant, the energy scale for an electron spectrum will be linear. This procedure is extremely useful in precise separation measurements of energy spectra. However, electrons with different initial energies will be either preaccelerated or decelerated by different amounts before entering the analyzer which may affect the relative heights of the spectral lines since the electron collection efficiency of the lens changes with voltage. By setting $C=1$ one can easily determine whether the magnetic field inside an analyzer is zero.[20]

For the cylindrical mirror analyzer the analyzer constant $C=[(\ln(b/a)]k^{-1}$ can be evaluated by measuring the analyzer dimensions a, b, z_0, d, and θ and then numerically solving the equation

$$z_0-d\cot\theta-4a\sqrt{k}\cos\theta e^{k\sin^2\theta}\int_0^{\sqrt{k}\sin\theta}e^{-u^2}du=0. \qquad (14)$$

Note that d and z_0 are not, of course, independent of one another.

TABLE I. Design parameters for the cylindrical mirror analyzer with second order focusing. (All lengths are in units of the inner cylinder radius a.)

d	θ (deg)	$\left(\frac{b}{a}\right)^{E/V_d}$	z_0	D	$\frac{\partial^2 z}{\partial\theta^2}(a/\text{rad}^2)$
0.01	30.164	1.0199	0.0516	0.0345	−0.9444
0.10	31.518	1.1935	0.4888	0.3363	−8.3136
0.20	32.805	1.3752	0.9282	0.6569	−14.9214
0.30	33.911	1.5466	1.3311	0.9663	−20.5913
0.40	34.875	1.7092	1.7059	1.2673	−25.7111
0.50	35.723	1.8643	2.0585	1.5616	−30.4912
0.60	36.477	2.0128	2.3931	1.8506	−35.0527
0.70	37.153	2.1557	2.7126	2.1350	−39.4686
0.80	37.763	2.2936	3.0195	2.4157	−43.7849
0.90	38.318	2.4272	3.3155	2.6931	−48.0311
1.00	38.825	2.5569	3.6022	2.9675	−52.2275
1.20	39.724	2.8061	4.1516	3.5090	−60.5209
1.40	40.497	3.0438	4.6748	4.0421	−68.7338
1.60	41.173	3.2721	5.1767	4.5683	−76.9019
1.80	41.772	3.4922	5.6608	5.0886	−85.0458
2.00	42.307	3.7054	6.1298	5.6038	−93.1776
2.20	42.790	3.9126	6.5859	6.1146	−101.3046
2.40	43.229	4.1144	7.0306	6.6216	−109.4316
2.60	43.631	4.3114	7.4654	7.1250	−117.5617
2.80	44.001	4.5041	7.8912	7.6254	−125.6969
3.00	44.344	4.6930	8.3090	8.1229	−133.8389
3.50	45.101	5.1505	9.3232	9.3561	−154.2276
4.00	45.746	5.5902	10.3010	10.5763	−174.6715
4.50	46.306	6.0152	11.2489	11.7858	−195.1733
5.00	46.799	6.4277	12.1716	12.9865	−215.7336
5.50	47.238	6.8295	13.0727	14.1795	−236.3523
6.00	47.634	7.2219	13.9550	15.3659	−257.0282
7.00	48.322	7.9828	15.6718	17.7220	−298.5471
8.00	48.903	8.7170	17.3352	20.0600	−340.2789
9.00	49.405	9.4292	18.9548	22.3832	−382.2128
10.00	49.846	10.1228	20.5373	24.6942	−424.3391
12.00	50.588	11.4641	23.6109	29.2874	−509.1318
14.00	51.196	12.7557	26.5855	33.8503	−594.5889
16.00	51.710	14.0074	29.4808	38.3904	−680.6586
18.00	52.152	15.2261	32.3104	42.9122	−767.2908
20.00	52.539	16.4169	35.0842	47.4195	−854.4479
30.00	53.958	22.0616	48.3346	69.8109	−1297.0468
40.00	54.901	27.3532	60.8757	92.0628	−1749.0326
50.00	55.597	32.4104	72.9434	114.2443	−2208.5996
60.00	56.144	37.2957	84.6624	136.3872	−2674.5385
70.00	56.592	42.0473	96.1090	158.5093	−3145.9976
80.00	56.969	46.6904	107.3338	180.6211	−3622.3324
90.00	57.294	51.2429	118.3728	202.7284	−4103.0277
100.00	57.579	55.7181	129.2530	224.8369	−4587.7032

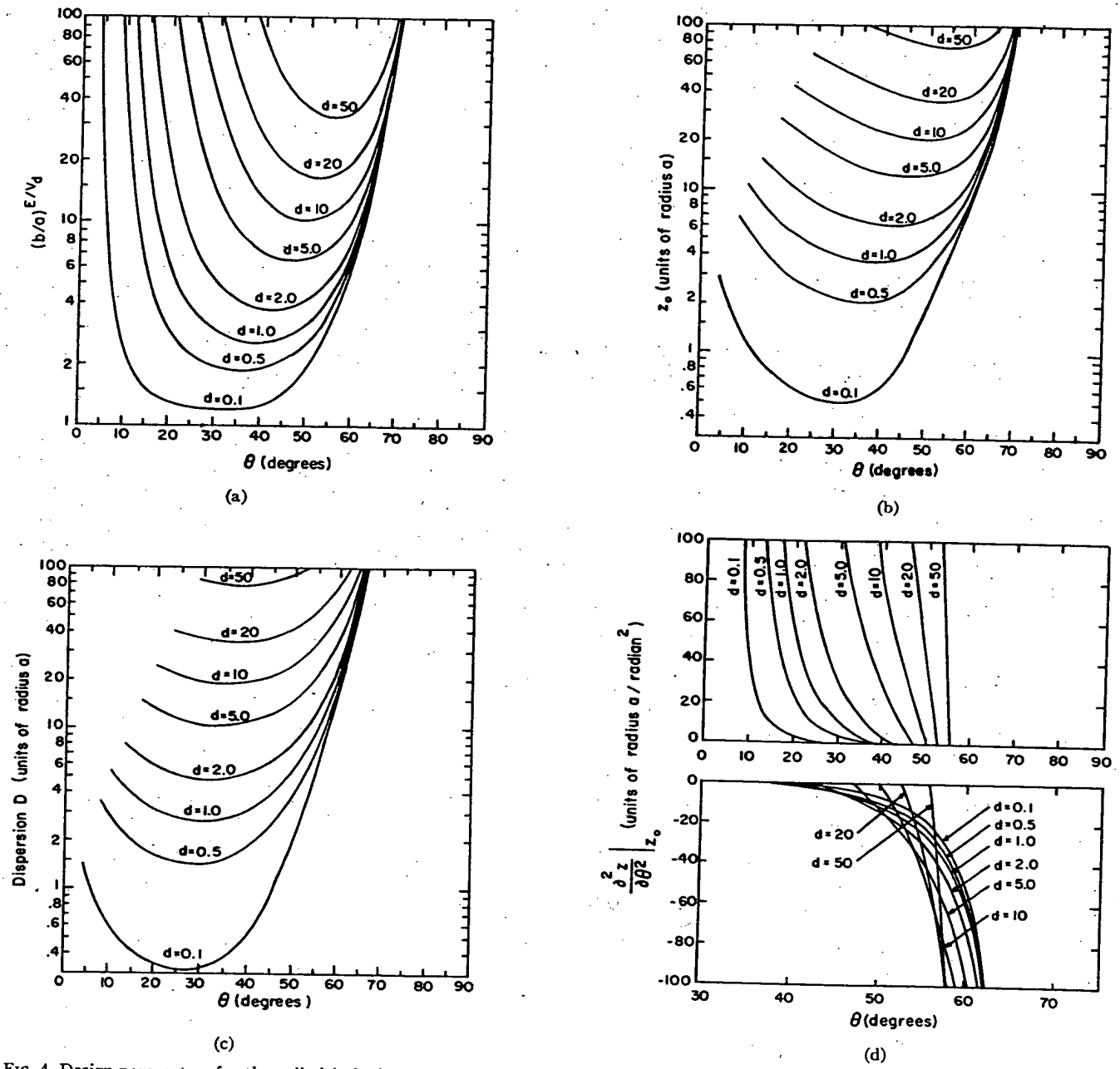

FIG. 4. Design parameters for the cylindrical mirror analyzer with first order focusing as a function of the entrance angle θ. The length d is in units of radius a. (a) ratio of cylinder radii, (b) z component of the electron trajectory, (c) dispersion, and (d) $\partial^3 z/\partial\theta^3$.

DESIGN PARAMETERS

Second Order Focusing

The optimum transmission for the cylindrical mirror analyzer occurs for second order focusing. For each source–image location d, this requires evaluating numerically the entrance angle θ, $(b/a)^{E/V_d}$, and z_0 for the condition

$$\partial z/\partial\theta = \partial^2 z/\partial\theta^2 = 0. \tag{15}$$

These design parameters are tabulated in Table I along with the dispersion and $\partial^3 z/\partial\theta^3$ so that one may calculate the base resolution using Eq. (13). In using Table I, one simply chooses the total source–image distance d from the inside surface of the inner cylinder. The remaining design parameters, then, are fixed. If one has complete design freedom, the least degradation occurs for $d=3a$ since the absolute value of the aberration constant $(3!D)^{-1}\partial^3 z/\partial\theta^3$ has a minimum there of $2.746a/\text{rad}^3$. On the other hand, this aberration term varies little with d reaching a maxi-

mum of $4.1a/\text{rad}^3$ and $3.4a/\text{rad}^3$ for $d=0.1a$ and $100a$, respectively.

First Order Focusing

In some experimental configurations it may be desirable to use both the complete 2π azimuthal acceptance angle and also a large range of entrance angles. For example, one may wish to measure the relative angular distributions of several electron peaks due to ion–gas collisions. If the unknown electron angular momentum associated with a peak is greater than unity, e.g., p, d, or f electrons, careful discrimination of the relative peak heights is necessary at several angles in order to determine the unknown angular momentum of the electrons. The requirements for second order focusing are quite restrictive. If the source and image lie completely within a closed cylinder and if second order focusing is used, then θ ranges between 30 and 45°. However, if one can limit the entrance acceptance angle so that first order focusing will be sufficient so as not to seriously degrade the base resolution ($\partial^2 z/\partial\theta^2 \neq 0$), then the range can be easily extended from 10 to 70°. The design parameters for first order focusing are shown as parametric curves in Fig. 4. The partial derivative $\partial^2 z/\partial\theta^2$ and the dispersion are included in these graphs for predicting the resolution. The usual case in ion collision experiments specifies that $d \leq 2a$ if one wishes to use the complete azimuthal angle.

COMPARISON OF SECOND ORDER FOCUSING WITH A PARALLEL PLATE ANALYZER AND A CYLINDRICAL MIRROR ANALYZER

Green and Proca[10] have shown that the parallel plate analyzer can have second order focusing. This result may be surprising; however, the equations describing the trajectory of electrons inside a cylindrical mirror and in a parallel plate analyzer are quite similar, and when both analyzers are properly designed, second order focusing can be achieved.

It is interesting to compare Eq. (2) with the much less complicated equation for a parallel plate analyzer. Using Fig. (2) to define similar dimensions, the total distance an electron travels along the z axis for a constant electric field is

$$z_0=(d_s+d_i)\cot\theta+2(E/V_d)h\sin 2\theta, \tag{16}$$

where h is the plate separation. The first term in this equation allows one the freedom to operate the parallel plate analyzer with second order focusing. That is, since two of the three variables are independent (θ, d_s+d_i, and h), one can adjust two of them so that both

$$\partial z/\partial\theta=0 \quad \text{and} \quad \partial^2 z/\partial\theta^2=0. \tag{17}$$

For the parallel plate analyzer the partial derivatives are

$$\begin{aligned}
\frac{\partial z}{\partial\theta}&=-d\sin^{-2}\theta+4h\frac{E}{V_d}\cos 2\theta,\\
\frac{\partial^2 z}{\partial\theta^2}&=2d\sin^{-3}\theta\cos\theta-8h\frac{E}{V_d}\sin 2\theta,\\
\frac{\partial^3 z}{\partial\theta^3}&=-2d(1+2\cos^2\theta)\sin^{-4}\theta-16h\frac{E}{V_d}\cos 2\theta,
\end{aligned} \tag{18}$$

and the dispersion is

$$D=2h(E/V_d)\sin 2\theta. \tag{19}$$

Second order focusing occurs only for $\theta=30°$ and for

$$d=d_s+d_i=\tfrac{1}{2}h(E/V_d). \tag{20}$$

The base resolution in this case is

$$R=\frac{w_{s_s}+w_{e_s}}{\sqrt{3}h(E/V_d)}-\frac{8}{3}\sqrt{3}[(+\Delta\theta)^3-(-\Delta\theta)^3]. \tag{21}$$

Comparing this result for the aberration constant $R(\Delta\theta)=|(3!D)^{-1}\partial^3 z/\partial\theta^3|$ with the cylindrical mirror analyzer, one finds that the parallel plate analyzer has a larger degradation in resolution due to a finite acceptance angle spread. For the parallel plate analyzer the aberration constant is

$$R(\Delta\theta)=4.6\ \text{rad}^{-3} \text{ at } \theta=30°.$$

For the cylindrical mirror analyzer,

$$R(\Delta\theta)=2.8\ \text{rad}^{-3} \text{ for } d=3a \text{ at } \theta=44.3°.$$

Not only does the cylindrical mirror analyzer have better transmission than the parallel plate analyzer with second order focusing, but it also disperses the energy more. Thus, for comparable dimensions the cylindrical mirror analyzer is capable of higher resolving power. For example, suppose one compares a cylindrical mirror analyzer with $d=3a$, $z_{0_{cm}}=8.3a$, $D_{cm}=8.1a$, and $b/a=4.7$ (see Table I) and a parallel plate analyzer with $z_{0_{pp}}=\frac{3}{2}\sqrt{3}h$ and $D_{pp}=\sqrt{3}h$ assuming for convenience that $E=V_d$ and that the appropriate dimensions for comparison are the radius of the outer cylinder b and the plate separation h. In order to make the analyzers comparable, one sets $z_{0_{cm}}=z_{0_{pp}}$ and finds that $h=0.68b$. Therefore, D_{cm} is 1.46 times larger than D_{pp} and the base resolution for the cylindrical mirror analyzer using Eq. (13) will be better for the same slit width sizes.

The most common parallel plate analyzer[21] is designed with the source and image defined by the entrance and exit slits in the analyzer's front plate; therefore, $d_s+d_i=0$ and only first order focusing is achieved because for $\theta=45°$,

$$\partial^2 z/\partial\theta^2=-8hE/V_d. \tag{22}$$

Also,

$$\partial^3 z/\partial\theta^3=0 \quad \text{at} \quad 45°. \tag{23}$$

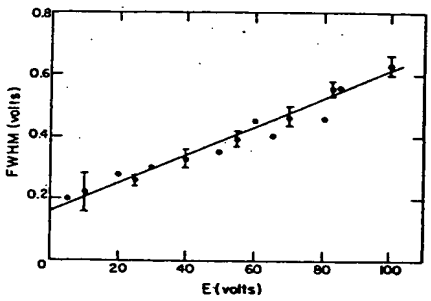

FIG. 5. Full width at half-maximum vs electron energy. The straight line is a linear least squares fit to the experimental data weighted by the number of measurements taken at each point. The linear increase in the FWHM is predicted by Eq. (13).

EXPERIMENTAL ANALYZER

Our cylindrical mirror analyzer was used to measure the electron spectra produced in H^-–gas target collisions. In addition to testing the analyzer with a beam of electrons from a hot cathode source, we have used several peaks in the continuous electron spectrum from H^- collisions. These lines are identified as autodetaching states of H^- produced during a collision of H^- with a neutral gas atom.[22]

The analyzer resolution was measured using a beam of electrons from a cathode ray tube assembly. The initial energy of the electrons was 30 eV with an FWHM of approximately 0.2 eV. In order to determine the resolution, the electron energy E was changed by preaccelerating or decelerating the electrons before they entered the field of the analyzer. This was accomplished by adjusting the voltage of the inner cylinder.[20,23] Equation (13) shows that the spread in electron energies ΔE will increase linearly with increasing electron energy E. The energy spread we measured was the FWHM. Figure 5 illustrates the measured linear relationship between the FWHM and the energy of the electrons. The straight line was determined from a linear least square fit to the experimental data with each point weighted according to the number of determinations made. The slope of this line is the value usually quoted for the experimental resolution.

$$\text{FWHM}=(0.0045\pm0.0002)E+(0.16\pm0.01). \quad (24)$$

Figure 6 exhibits the measured electron energy distribution for several analyzing energies E. The electron gun from a CRT was used for the source of electrons. Since the distribution was triangular with rounded corners, except at very low analyzing energies, the base resolution was exactly twice the FWHM resolution. Therefore, the measured base resolution is

$$R=0.0090\pm0.0004. \quad (25)$$

This result is in excellent agreement with the predicted base resolution shown below in Eq. (30).

The dimensions of our experimental analyzer were

$$\begin{aligned} &d=2a && z_0=7.772\pm0.013 \text{ cm},\\ &a=1.270\pm0.003 \text{ cm}, && \theta=42.5°,\\ &b=4.717\pm0.003 \text{ cm}, && \Delta\theta=\pm1.0°,\\ &w_s=0.023\pm0.003 \text{ cm}, && w_e=0.017\pm0.001 \text{ cm},\\ &r_c=0.023 \text{ cm}. \end{aligned} \quad (26)$$

The calculated analyzer constant was 1.0031 ± 0.0045. By measuring the effect of a magnetic field in our analyzer, an experimental determination showed[20]

$$C=0.9995^{+0.0005}_{-0.0019}.$$

At $\theta=42.5°$, the dispersion is $5.642a$ using Fig. 4. With these values for our analyzer and using Eq. (13), one finds that

$$\begin{aligned} R(w_{s_z},w_{e_z})&=0.0083\pm0.0011,\\ R(r_c)\quad\ &=0.0003. \end{aligned} \quad (27)$$

Using Eq. (8) to find Δz_T,

$$\Delta z(\Delta\theta)\simeq\frac{1}{2!}\frac{\partial^2 z}{\partial\theta^2}(\Delta\theta)^2+\frac{1}{3!}\frac{\partial^3 z}{\partial\theta^3}(\Delta\theta)^3+\cdots. \quad (28)$$

From Fig. 4 and Table I,

$$\frac{\partial^2 z}{\partial\theta^2}=-0.3a/\text{rad}^2, \quad \frac{\partial^3 z}{\partial\theta^3}=-97a/\text{rad}^3.$$

For our acceptance angle $\Delta\theta=\pm1.0°$, one finds

$$\begin{aligned} \Delta z(+\Delta\theta)&=-1.3\times10^{-4}a,\\ \Delta z(-\Delta\theta)&=0.4\times10^{-4}a, \end{aligned} \quad (29)$$

and

$$\Delta z_T(+\Delta\theta,-\Delta\theta)=1.7\times10^{-4}a.$$

Clearly, the angular aberrations produce a negligible effect and

$$R=0.0086\pm0.0011. \quad (30)$$

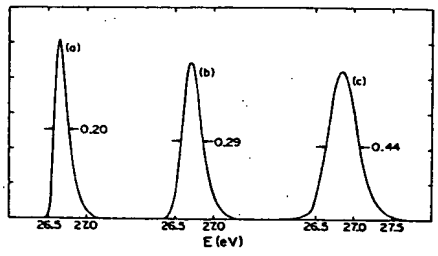

FIG. 6. X–Y recorder tracing of the electron energy distribution. The initial electron energy was ~27 eV before entering the analyzer. Voltage between the inner and outer cylinders determined the analyzing energy. The analyzing energy was 5 eV for (a), 30 eV for (b), and 60 eV for (c). The asymmetry in the low energy peak (a) is probably due to the Maxwellian distribution of electrons from the hot cathode.

As seen here, in the case of small acceptance angles the resolution is completely determined by the finite slit-widths. The angular term in Eq. (29) equals the slitwidth term only when $\Delta\theta$ is increased to $\pm 9°$. Therefore, in all experiments with small acceptance angles, it may be necessary only to utilize first order focusing for good resolution rather than to restrict the experimental arrangement to second order configurations for the cylindrical mirror analyzer.

ACKNOWLEDGMENTS

The author wishes to acknowledge Dr. Alan K. Edwards for his help in the design, construction, and operation of the cylindrical mirror analyzer. He is also grateful to Dr. Ron H. McKnight for his critical review of this manuscript and to Professor Ronald Geballe for his support and encouragement.

APPENDIX

For completeness, the energy dispersion and the first three partial derivatives of z with respect to θ for the cylindrical mirror analyzer are listed below:

$$D=E\partial z/\partial E=ak\sin 2\theta + (2ak^{\frac{1}{2}}\cos\theta+4ak^{\frac{1}{2}}\cos\theta\sin^2\theta)WI, \quad \text{(A1)}$$

$$\partial z/\partial\theta=-d\sin^{-2}\theta+4ak\cos^2\theta + (8ak^{\frac{1}{2}}\sin\theta\cos^2\theta-4ak^{\frac{1}{2}}\sin\theta)WI, \quad \text{(A2)}$$

$$\partial^2 z/\partial\theta^2=2d\sin^{-3}\theta\cos\theta-12ak\cos\theta\sin\theta+8ak^2\sin\theta\cos^3\theta + (8ak^{\frac{1}{2}}\cos^3\theta-24ak^{\frac{1}{2}}\sin^2\theta\cos\theta-4ak^{\frac{1}{2}}\cos\theta + 16ak^{\frac{1}{2}}\sin^2\theta\cos^3\theta)WI, \quad \text{(A3)}$$

$$\partial^3 z/\partial\theta^3=-6d\sin^{-4}\theta\cos^2\theta-2d\sin^{-2}\theta+12ak\sin^2\theta - 16ak\cos^2\theta+16ak^2\cos^4\theta-48ak^2\sin^2\theta\cos^2\theta + 16ak^3\sin^2\theta\cos^4\theta+(-80ak^{\frac{1}{2}}\sin\theta\cos^2\theta+24ak^{\frac{1}{2}}\sin^3\theta + 4ak^{\frac{1}{2}}\sin\theta+48ak^{\frac{1}{2}}\sin\theta\cos^4\theta-96ak^{\frac{1}{2}}\sin^3\theta\cos^2\theta + 32ak^{7/2}\sin^3\theta\cos^4\theta)WI, \quad \text{(A4)}$$

where

$$W=\exp(k\sin^2\theta), \quad I=\int_0^{\sqrt{k}\sin\theta} e^{-u^2}du,$$

and $k=(E/V_d)\ln(b/a)$. The definite integral I was evaluated using a polynomial approximation.[24]

* This work was supported in part by the Army Research Office, Durham, N. C.

† NASA Predoctoral trainee.

[1] V. V. Zashkvara and V. S. Red'kin, Sov. Phys. Tech. Phys. **14**, 1089 (1970).
[2] S. Aksela, M. Karras, M. Pessa, and E. Suoninen, Rev. Sci. Instrum. **41**, 351 (1970).
[3] H. Z. Sar-El, Rev. Sci. Instrum. **38**, 1210 (1967).
[4] V. V. Zashkvara, M. I. Korsunskii, and O. S. Kosmachev, Sov. Phys. Tech. Phys. **11**, 96 (1966).
[5] R. Gremmelmaier, dissertation, Karlsruhe, 1952.
[6] H. Z. Sar-El, Rev. Sci. Instrum. **39**, 533 (1968).
[7] F. R. Paolini and G. C. Theodoridis, Rev. Sci. Instrum. **38**, 579 (1967); see also references therein to earlier papers.
[8] H. Hafner, J. Arol Simpson, and C. E. Kuyatt, Rev. Sci. Instrum. **39**, 33 (1968).
[9] H. Z. Sar-El, Rev. Sci. Instrum. **41**, 561 (1970).
[10] T. S. Green and G. A. Proca, Rev. Sci. Instrum. **41**, 1409 (1970).
[11] E. Blauth, Z. Physik **147**, 228 (1957).
[12] W. Mehlhorn, Z. Physik **160**, 247 (1960); **187**, 21 (1965).
[13] G. N. Ogurtsov, I. P. Flaks, and S. V. Avakyan, Sov. Phys. Tech. Phys. **14**, 972 (1970).
[14] G. N. Ogurtsov, I. P. Flaks, and S. V. Avakyan, Sov. Phys. JETP **30**, 16 (1970); Sov. Phys. Tech. Phys. **15**, 876 (1970); **15**, 1656 (1971).
[15] E. Harting, Rev. Sci. Instrum. **42**, 1151 (1971).
[16] G. Vassilev, J. Baudon, G. Rahmat, and M. Barat, Rev. Sci. Instrum. **42**, 1222 (1971).
[17] R. W. Hayward, Advan. Electron. **5**, 97 (1953).
[18] S. Aksela, Rev. Sci. Instrum. **42**, 810 (1971).
[19] G. A. Proca and T. S. Green, Rev. Sci. Instrum. **41**, 1778 (1970).
[20] J. S. Risley, Rev. Sci. Instrum. **42**, 267 (1971).
[21] G. A. Harrower, Rev. Sci. Instrum. **26**, 850 (1955).
[22] J. S. Risley, A. K. Edwards, and R. Geballe (to be published).
[23] M. E. Rudd, Rev. Sci. Instrum. **37**, 971 (1966).
[24] M. Abramowitz and I. A. Stegun, *Handbook of Mathematical Functions* (Dover, New York, 1965), Sec. 26.2.19, p. 932.